GEOLOGICA BELGICA (2010) 13/4: 345-360

THE GIVETIAN-FRASNIAN BOUNDARY AT NISMES PARASTRATOTYPE (BELGIUM): THE MAGNETIC SUSCEPTIBILITY SIGNAL CONTROLLED BY FERROMAGNETIC MINERALS

Xavier DEVLEESCHOUWER[1,2], Estelle PETITCLERC[1], Simo SPASSOV[3] & Alain PRÉAT[2]

(10 figures, 1 table)

[1]Royal Belgian Institute of Natural Sciences, Geological Survey of Belgium, 13 Rue Jenner, B-1000 Brussels, Belgium. E-mail : Xavier.Devleeschouwer@naturalsciences.be , Estelle.Petitclerc@naturalsciences.be
[2]Department of Earth and Environmental Sciences, Sedimentology and Basin Analysis, Université Libre de Bruxelles CP 160/02, 50 av F.D Roosevelt, B-1050 Brussels, Belgium. E-mail : apreat@ulb.ac.be
[3]Royal Meteorological Institute of Belgium, Centre de Physique du Globe, Section du Magnétisme Environnemental, B-5670 Dourbes (Viroinval), Belgium. E-mail: simo.spassov@oma.be

ABSTRACT. A comparison between microfacies and magnetic susceptibility (MS) curves has been performed at the Givetian-Frasnian transition in southern Belgium. The MS curve is subdivided in four magnetic sequences. Most of the section has MS and MF curves anti-correlated. Hysteresis parameters reveal a low coercivity mineral of magnetite type phase and a high coercivity mineral (i.e. hematite) in all samples. Strong correlation between ferromagnetic and low-field magnetic susceptibilities suggests that ferromagnetic minerals control almost totally the MS signal with an increasing upsection abundance of paramagnetic grains (iron-bearing clay minerals and pyrite). A decreased proportion of superparamagnetic grains, probably of diagenetic origin, is observed upsection. The hematite grains increases in the Frasnian as attested by the higher hematite contribution to the IRM_{500mT}. The anti-correlation between the magnetic viscosity coefficient and the hematite contribution to the IRM_{500mT} suggest that hematite are not associated to the superparamagnetic fraction and has a detrital origin. The opposite evolutions could be partly explained by sedimentological parameters and by an increased amount of primary detrital magnetite and hematite upsection. This detrital influx highlights the drowning of the carbonate platform at the end of the Givetian illustrating the progressive change from a Givetian rimmed platform towards a Frasnian ramp setting.

KEYWORDS: Givetian-Frasnian boundary, magnetic susceptibility, microfacies, hysteresis curve, viscosity index.

1. Introduction

Whole-core magnetic susceptibility (MS) logging of deep-sea sediments, mainly for high-resolution lithostratigraphic correlation, has become a routine procedure on all Ocean Drilling Program (ODP) cruises since ODP Leg 108 in 1986 (Bloemendal et al., 1989). MS data were used mainly in the Quaternary to identify glacial and interglacial sequences. During the nineties, MS studies were applied to older rocks such as the Devonian carbonates series of the Tafilalt and Mader basins (Crick et al., 1994) and the Upper Devonian (Frasnian-Famennian boundary) in Europe (Devleeschouwer, 1999; Devleeschouwer et al., 1999). The detrital fraction changes in the sedimentary rocks constitute the major source of the MS variations (Ellwood et al., 2000), which are related to the changes in terrigenous clastic sediment supply from continental sources to the marine realm (Crick et al., 2001). These MS evolutions are basically explained by sea-level oscillations with high MS values during regressions implying an increase of erosion on exposed continental masses, leading to higher quantities of detrital minerals transported into the marine realm. On the contrary, low MS values are recorded during transgressive episodes (Crick et al., 1997, 2000, 2001). Increasing detrital inputs to the marine domain will enhance the MS signal due to higher magnetic grain abundance. Different sources of uncarbonated, mostly terrigenous components are known and relate to riverine-fluviatile (Crick et al., 2000, 2001), volcanic activities (Gorbarenko et al., 2002), hydrothermal vents (Borradaile & Lagroix, 2000), bolide impacts (Ellwood et al., 2003), eolian supply (Hladil, 2002; Hladil et al., 2006 and this volume) and pedogenetic minerals during the formation of paleosols (Chen et al., 2005).

MS fluctuations are considered as a potential high-resolution stratigraphic tool to correlate sedimentary sections inside the same basin or even between different basins (Ellwood et al., 2001, 2007, 2008). The use and the comprehension of the MS evolutions in the Paleozoic sedimentary series without a control on the evolution of the microfacies could often lead to misunderstandings. The identification of the different microfacies and their evolution along the section will help to determine: (1) the depositional environments, (2) the sedimentological aspects and (3) the variations of these parameters in function of the stratigraphical timeline.

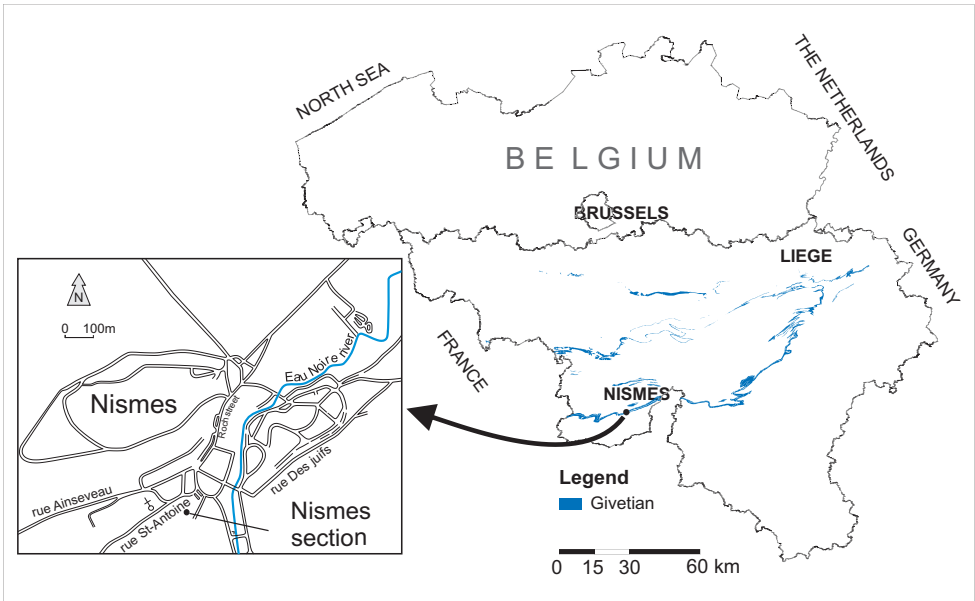

Figure 1. Locality map of the Givetian-Frasnian Nismes section.

The Nismes section is one of the several outcrops studied in a research project aimed at comparing sedimentological analysis (microfacies) and magnetic susceptibility curves in the Givetian carbonate platform across Belgium and neighbouring countries. One of the purposes of this study is to establish a detailed and high-resolution low-field magnetic susceptibility stratigraphy of the Givetian series in Belgium (see also Boulvain et al., this volume). MS curves will be used for correlating different Belgian sections between them and to possibly establish correlations with international stratotype and GSSP sections in France (Puech de la Suque section, Casier & Préat, 2007 and references therein) and Morocco (Walliser et al., 1995, Bultynck, 1987). Other sections are under study at the Givetian-Frasnian boundary in Belgium (Sourd d'Ave, Flohimont, Sy) and at the base of the Givetian (Trois-Fontaines and Terres d'Haurs Formations, Casier et al., 2009; Devleeschouwer et al., 2009).

The different objectives of this paper concern the characterization of the MS curve evolution along the lithological column, the comparison of the MS curve with the microfacies, the investigation of the magnetic mineralogy using thermomagnetic measurements and hysteresis parameters. These analyses will be used to determine (1) the magnetic mineral populations controlling the MS signal, (2) their grain size classes and (3) the estimation of a preserved primary magnetic signal. These data will permit to discuss further in details the evolution of the MS signal and its use as a tool to depict the sea-level oscillations at the Givetian-Frasnian boundary in Belgium.

2. Location and geological context

2.1. Geographical and geological setting

The Nismes section (50° 04' N, 4° 32' E) is located 250 m SW of the Nismes village, in the southern part of the allochthonous Ardennes fold-and-thrust belt (southern Belgium) about 22 km SW of Givet and 2.85 km east of Frasnes (Fig. 1). The Nismes section was adopted by the Subcommission on Devonian Stratigraphy (SDS) (Prague, 1986) as an auxiliary stratotype for the Givetian-Frasnian boundary in a neritic facies (Bultynck et al., 1988b). It exposes 26 meters belonging to the upper part of the Fromelennes Formation (Late Givetian) and the stratotype for the base of the Nismes Formation (Late Givetian and Early Frasnian) (Bultynck, 1987; Bultynck et al., 1988a; Boulvain et al., 1999). The lower most 15 m correspond to the upper part of the Fort Hulobiet Member, which belongs to the Fromelennes Formation (Fig. 2). In the Nismes section, the Fromelennes Formation consists of thin to medium bedded fine-grained homogeneous greyish limestones with abundant crinoids and brachiopods in its upper part. The second part of the section starts with the Pont d'Avignon Member consisting of 1.4 meter thick nodular limestones with very abundant brachiopods. The Pont d'Avignon Member is overlain by the Sourd d'Ave Member (only 11 meters are exposed) showing greenish or brownish shales with a few carbonate nodules at the base and numerous calcareous lenses in the upper part. The Givetian-Frasnian boundary is fixed on the base of the first appearance of the conodont species *Ancyrodella rotundiloba* in the basal part of the Sourd d'Ave Member (Bultynck et al., 1988). The internationally accepted GSSP section for the Givetian-Frasnian boundary is located in Puech de la Suque (Montagne Noire, France), which was described by Klapper et al. (1987) and placed at the first occurrence of an early morphotype of the conodont *Ancyrodella rotundiloba.* This species appears slightly above the base of the Nismes Formation in many sections of the Ardennes (Bultynck et al., 1988). More recently, Casier & Préat (2009) have suggested displacing the Givetian-Frasnian boundary to a lower level close to the end of the Fromelennes Formation as indicated by concomitant changes in term of ostracod assemblages and microfacies evolution.

The stratification of the series is not affected by faults or folding. In total, 94 samples were systematically collected every 15-30 cm for magnetic susceptibility measurements through all the lithologies including limestones, carbonate nodules and shales. 16 samples were selected for detailed rock magnetic analyses.

2.2. Microfacies analysis

A detailed microfacies analysis, recently carried out by Casier & Préat (2009), in the upper part of the Fromelennes Formation and in the basal part of the Nismes Formation is summarized here. The microfacies curve (Fig. 2, column 4) corresponds to the Préat and Mamet's standard sequence (1989) composed of 13 microfacies even if the microfacies MF4, MF5 and MF7 have not been observed in the Nismes section. Open-marine environment, below or within the storm wave base, corresponds to clayey and silty microbioclastic mudstones and wackestones (MF1) to laminar bioclastic packstones with crinoids, brachiopods, ostracods, molluscs, a few bryozoans and tentaculitoids (MF3). The presence of bioclastic laminae ranging in size from thin (< 1 mm) to thick (> 0.5 cm) and the evolution from parallel to oblique laminations are indicative of episodic tempestites recording a distal (MF1) to proximal (MF3) gradient in a shallow mixed siliciclastic-carbonate shelf. This environment is present only in microfacies sequences 3 and 5.

An open-marine peri-reefal environment, near or within the fair-weather wave base, is observed for MF6, which consists of coral floatstones and rudstones with microbreccias, gastropods, bivalves, ostracods, a few brachiopods and peloids. Microfacies MF4, MF5 and

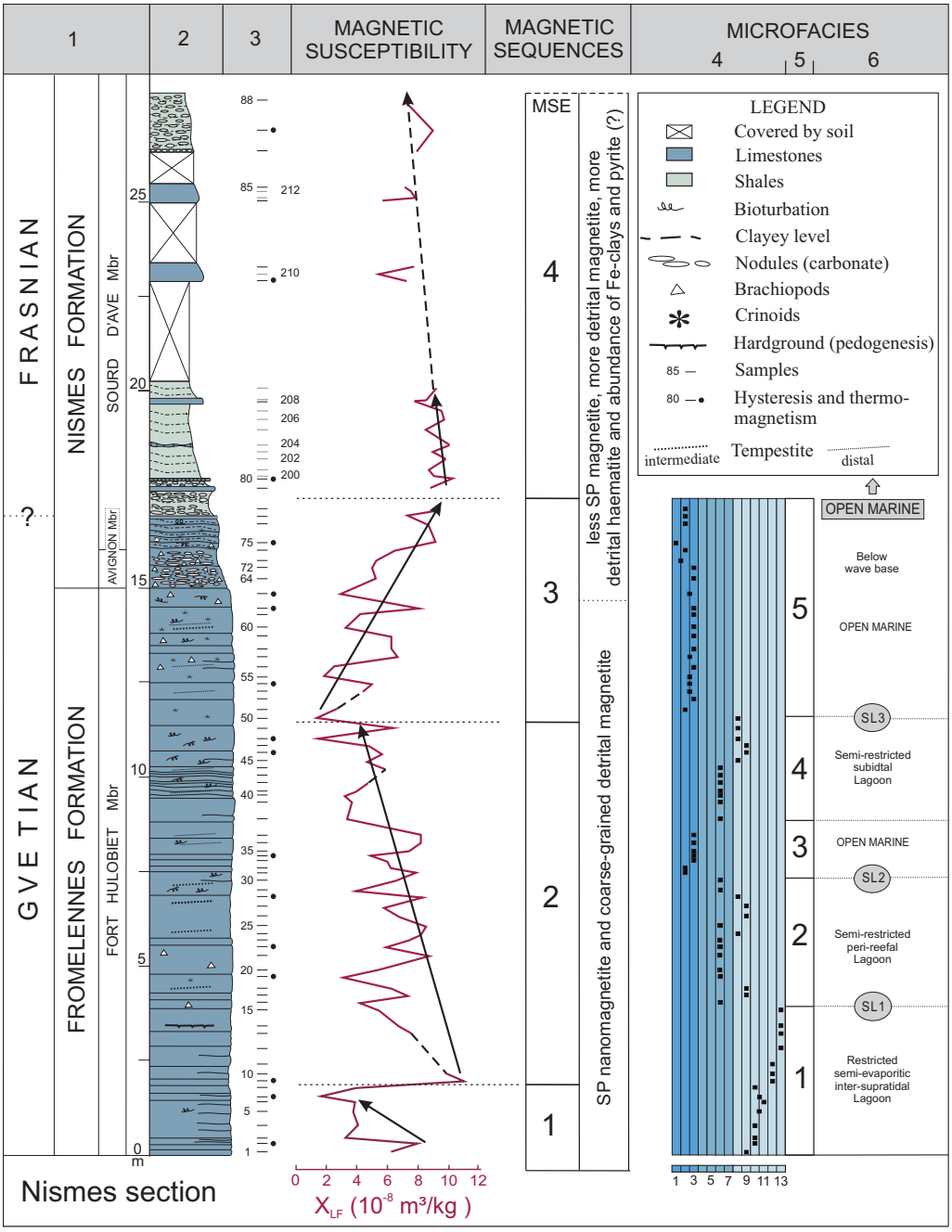

Figure 2. Lithological column of the Nismes section. Columns: (1) stratigraphy, (2) lithological column, (3) position of the samples collected for magnetic susceptibility (MS) analyses (those selected for hysteresis are marked with a black dot), MS curve, magnetic sequences. The first 78 magnetic susceptibility samples belong to the data set of Casier & Préat (2009). (4) microfacies standard sequence after Casier & Préat (2009), (5) sequences and (6) sedimentological and paleoenvironmental interpretations after Casier & Préat (2009). The MS curve contains four magnetic susceptibility evolutions (MSE) numbered from 1 to 4.

MF7 are not observed in the Nismes section. They represent in the Préat and Mamet's (1989) model the barrier belt environments dominated by reworked stromatoporoids, corals and algae. The absence of these microfacies at Nismes suggests that only small bioconstructions existed at that time on the shelf and no real reefal barrier environment (see also Préat et al., 2007).

Restricted lagoonal intertidal and supratidal environments with salinity fluctuations are recorded in the six successive microfacies MF8-13. They consist of mudstones and wackestones with issinellid packstones and bafflestones with abundant peloids and lumps (MF8-9). Spongiostromid packstones and bindstones contain abundant ostracods, few bivalves and calcispheres, irregular fenestrae and thin dessication cracks (MF10). Microsparitized peloidal packstones contain abundant bivalves, gastropods, ostracods and common cyanobacterial *Bevocastria* observed in lumps (MF11). Homogeneous mudstones with a few ostracods, molluscs and *Amphipora* (MF12) record near-emersion conditions and fine-grained dolomudstones reveal semi-evaporitic conditions (MF13).

The studied microfacies curve has been subdivided into five sequences separated by minor and major sea-level fluctuations (Fig. 2, columns 5-6). The first sequence shows a large regressive evolution corresponding to a shallowing-upward sequence in the restricted lagoonal environments from MF7 to MF13. A major sea-level rise is observed at the transition from sequences 1 to 2 as indicated by the large shift from semi-evaporitic (MF13) to peri-reefal conditions (MF6). A minor sea-level rise is observed at the transition towards the base of the next sequence as revealed by the change from peri-reefal (MF6) to distal open-marine conditions close to the storm wave base (MF2). The third sequence records briefly a deeper open-marine setting (MF1-3). The regressive evolution is still present in the next sequence (4), with the evolution of peri-reefal to intertidal lagoonal conditions. A major sea-level rise between sequence 4 and 5 highlights a rather abrupt change from a restricted lagoon to deep open-marine environment under the influence of storm activities. This environment encompasses the whole sequence 5 with a small transgressive evolution from microfacies (MF2-3) at the end of the Fromelennes Formation to microfacies (MF1-2) at the base of the Nismes Formation.

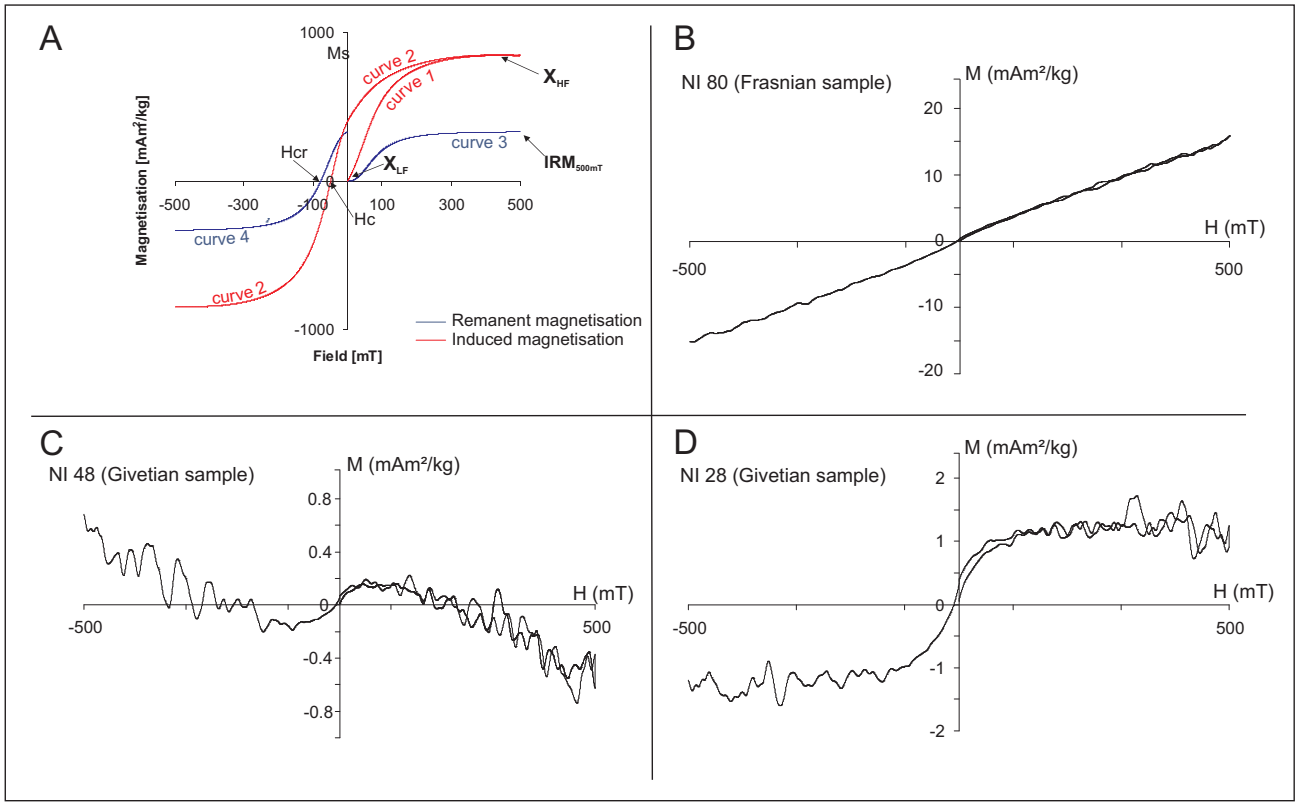

Figure 3. A) Sketch of magnetisation curve measurements performed with the J-coercivity meter. Curve 1 (red) represents the initial hysteresis curve and curve 2 (red) the descending branch of the hystersis loop. From these curves (slope-corrected) the saturation magnetisation M_s, the coercive force H_c and the high-field magnetic susceptibility X_{HF} are calculated. Curve 3 (black) represents the IRM acquisition from 0 to 500 mT and curve 4 (black) is the backfield curve between 0 and -500mT. Saturation magnetisation at 500 mT (IRM_{500mT}) and coercivity of remanence H_{cr} were obtained from remanence measurements. Typical hysteresis curves (uncorrected for the slope) for a sample from the Nismes sections containing ferrimagnetic plus paramagnetic minerals – sample Ni 80 from the Frasnian (B), ferrimagnetic and diamagnetic minerals – sample Ni 48 from the Givetian (C) and only ferrimagnetic minerals – sample Ni 28 from the Givetian (D).

3. Methodology

Magnetic susceptibility (MS) was measured at the Royal Belgian Institute of Natural Sciences with a MFK1-A susceptometer at room temperature in a low AC magnetic field of 400 A/m and at a frequency of 976 Hz. The MS values of the samples were corrected for the susceptibility of the empty plastic holder. Each sample was weighted with a precision of 0.01 g and measured three times and averaged. The masses involved range from 4.9 to 24.65 g. This procedure allows determining the mass specific low-field magnetic susceptibility (X_{LF}) of each sample, representing an integral over all dia-, para- and ferromagnetic contributions present in the rock.

Thermomagnetic analyses and hysteresis measurements were undertaken on 16 samples taking into account the entire MS variability, microfacies type and sedimentological characteristics. Thermomagnetic susceptibility measurements were realised using a CS3 furnace or high temperature control unit connected to the MFK1-A susceptometer. A powder sample (grain size < 150 μm) was heated progressively from room temperature to 700 °C and subsequently cooled down again to room temperature at a rate of 12 °C/min. The low-field MS was monitored during the whole cycle, which was performed in an argon atmosphere in order to prevent oxidation processes due to air oxygen.

The shape of a hysteresis curve is characteristic of the magnetic properties of the material and shows the ease with which it is magnetised and the ability to retain this magnetisation (Evans & Heller, 2003). Isothermal magnetisation curves were realized on a cuboid rock placed in a small paper box with a J-Coercivity "rotation" magnetometer developed by Kazan University (Burov et al., 1986) and sited at the Geophysical centre of the Royal Meteorological Institute. The magnetising field was increased every 0.5 mT from 0 to +500 mT, then decreased to zero and further decreased to –500 mT and induced and remanent magnetisation were measured at each field increment/decrement. Finally, the decay of the IRM_{500mT} was monitored for about 100 s. These measurements allowed the determination of the initial hysteresis curve (curve 1 in Fig. 3A), the descending branch of the hysteresis curve (curve 2 in Fig. 3A) as well as the Isothermal Remanent Magnetisation (IRM) acquisition (i.e. remanence from 0 to + 500 mT, curve 3 in Fig. 3A) and backfield curve (remanence from 0 to -500 mT, curve 4 in Fig. 3A). In order to calculate the *saturation magnetisation* M_s (mAm²/kg) and *coercive force* B_c (mT), a slope was fitted through the points between 400 and 500 mT of the hysteresis curve, which was then subtracted from it (slope correction). The slope at high-field corresponding to the high-field magnetic susceptibility (X_{HF}) is indicative for paramagnetic and diamagnetic contributions to the low-field magnetic susceptibility, if high coercivity minerals such as goethite and hematite are not present. The ferromagnetic susceptibility X_{Ferro} (m³/kg), corresponding to the ferromagnetic s.l. minerals, can be calculated by subtracting X_{HF} from X_{LF} (Walden et al., 1999). The saturation isothermal remanent magnetisation at 500 mT or IRM_{500mT} (mAm²/kg) and *coercivity of remanence* B_{cr} (mT) were obtained from the backfield curve (Fig. 3). The percentage of remanence decay is an indication for ultrafine magnetic grains near the superparamagnetic (SP) / single domain (SD) grain-size boundary, which is at room temperature about 30 nm for magnetite and hematite (Dunlop & Özdemir, 1997). The normalised magnetic viscosity coefficient was calculated from the remanence decay measured during 100 s.

4. Results of rock magnetic analyses

4.1. Magnetic Susceptibility curve

The X_{LF} values of the Nismes section are relatively low (between 1.36 and 10.5 x 10^{-8} m³/kg, Fig. 2) as usually observed for most of the carbonate rocks (between 1 x 10^{-9} and 1 x 10^{-7} m³/kg, Ellwood et al., 1999). The highest value is measured at the base of the section in the Fromelennes Formation. Despite low values, the MS signal fluctuates along the lithological column with several MS evolutions (MSE) reported as magnetic sequences. Four main MSE trends, numbered from 1 to 4, are seen in Fig. 2. MSE 1 and 2 in the Fort Hulobiet Member record two successive decreasing MS trends. MSE 2, over nearly 10 m, displays the largest X_{LF} amplitude fluctuation of the serie. The lowest X_{LF} value of the section is observed at the transition between MSE 2 and MSE 3. An increasing X_{LF} trend from 1.36 to 8.85 x 10^{-8} m³/kg is observed during MSE 3. Finally, MSE 4 shows distinctly at the base a small decreasing trend that seems to continue upwards in the discontinuous outcropping Frasnian shales and limestones.

4.2. Magnetic mineralogy

Thermomagnetic susceptibility measurement (TSM) curves illustrating two representative samples (Ni 54 and Ni 87, Fig. 4) show a very slight decrease between 23-200°C. A small peak between 400 and 580 °C is observed in most of the samples indicating magnetic mineral formation during the heating. The cooling curve of all samples shows a large increase between 580-400°C. The room temperature susceptibility after cooling down is much higher than before heating, probably due to neoformation of ferrimagnetic minerals, at high temperatures (Hrouda, 1994). Due to thermomagnetic alteration during heating the TSM curves cannot be used for characterisation of the original magnetic population.

The uncorrected hysteresis curve obtained for the 16 selected samples is clearly different between the Givetian and the Frasnian (Fig. 3 B-D). All samples (Ni 63, 75, 80, 83, 87) corresponding to the top of the Fromelennes Formation and the base of the Nismes Formation are characterized by a "sigmoid"–shaped loop that hardly opens at low fields (Fig. 3B). This hysteresis curve implies that the ferrimagnetism is largely masked by the presence of paramagnetic contribution. Two other forms of hysteresis curves are also observed only in the Givetian and show: (1) a large contribution of diamagnetic minerals

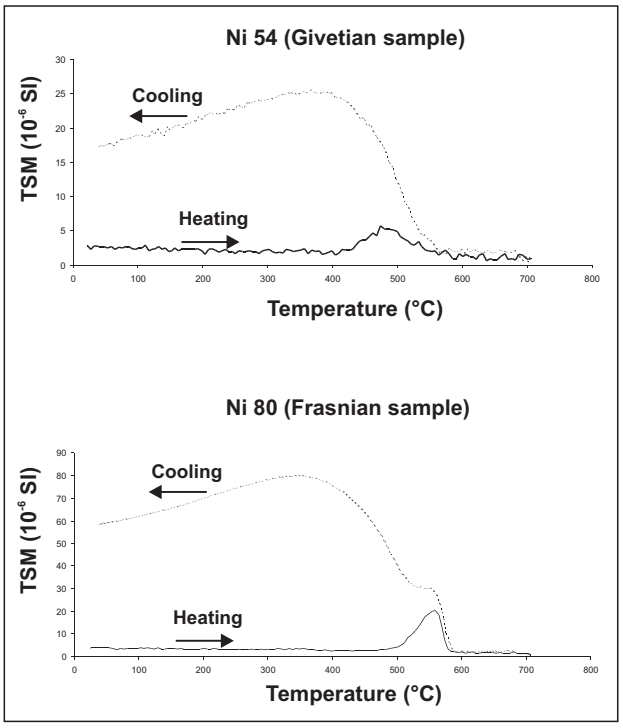

Figure 4. Bulk susceptibility changes upon heating and cooling (marked with arrows) for two samples: a Givetian limestone (Ni54) from the uppermost part of the Hulobiet Member and a Frasnian carbonate nodule (Ni87) from the Sourd d'Ave Member near the top of the section. The heating curves correspond to black lines and black-dashed lines represent the cooling curves.

(samples Ni 02, 07, 09, 46, 48, Fig. 3C) and (2) a hysteresis curve being evocative of a wasp-waisted shape (samples Ni 19, 22, 28, 34, 54, 62, Fig. 3D). Wasp-waisted curve shape may indicate mixtures of superparamagnetic and single-domain magnetite (Tauxe et al. 1996).

The majority of the samples have backfield curves such as seen in Fig. 5 (sample Ni 46), which are close to saturation at -300 mT, but show a small further decrease until -500 mT that makes up between 4 and 14 % of the IRM_{500mT}. However, for three of the sixteen samples this decrease is much stronger (e.g. Ni 80 in Fig. 5), the contribution to the IRM_{500mT} being above 19%. Apparently, high coercivity minerals are present with variable contributions to the IRM_{500mT}. It is assumed that hematite is responsible for the high field IRM contributions rather than goethite, because the latter is progressively transformed into hematite during moderate to strong diagenesis. Marine limestones and shales of the Nismes section underwent burial diagenesis as indicated by the conodont alteration index (CAI) ranging between 3 and 4 and the illite crystallinity index, which corresponds to temperatures between 120 and 190°C (Helsen 1992, Fielitz & Mansy, 1999). This falls into the temperature range where the goethite-hematite phase transition is initiated (Christensen et al., 2007) and given the age of the section, which is about 385 million years old after the 2009 version of the International Stratigraphic Chart published by the International Commission on Stratigraphy, it is rather unlikely that goethite has survived up to today. This is in agreement with studies of Berner (1969) and van Houten (1973) who investigated red beds. These authors proposed that poorly crystalline iron oxyhydroxides alter to hematite even at temperatures below 85°C occurring during shallow burial diagenesis. Moreover, goethite has been found in several oolitic ironstones from Late Ordovician (Yapp & Poths, 1993) and Jurassic ages (Yapp 1998). Natural goethite were also discovered as authigenic minerals formed in continental environments (soils) or in shallow subsurface environments (e.g. botryoidal or radiating masses in pockets or fissures in the rocks) (Yapp, 1987, 2000). These types of goethite-bearing ironstones were not observed in the present study of the marine limestones and shales at the Givetian-Frasnian boundary.

Fig. 6A shows the decay of the IRM_{500mT} expressed as normalized values relative to the IRM at 0 s (IRM_0) plotted against the time (s) on a logarithmic scale. One recognises that all the curves are of exponential nature but that the IRM loss is different for the two representative samples (Ni 19 – Givetian and Ni 87 – Frasnian). In general, between 7 and 13 % of the IRM_{500mT} are lost within 100 s indicating the presence of superparamagnetic and/or

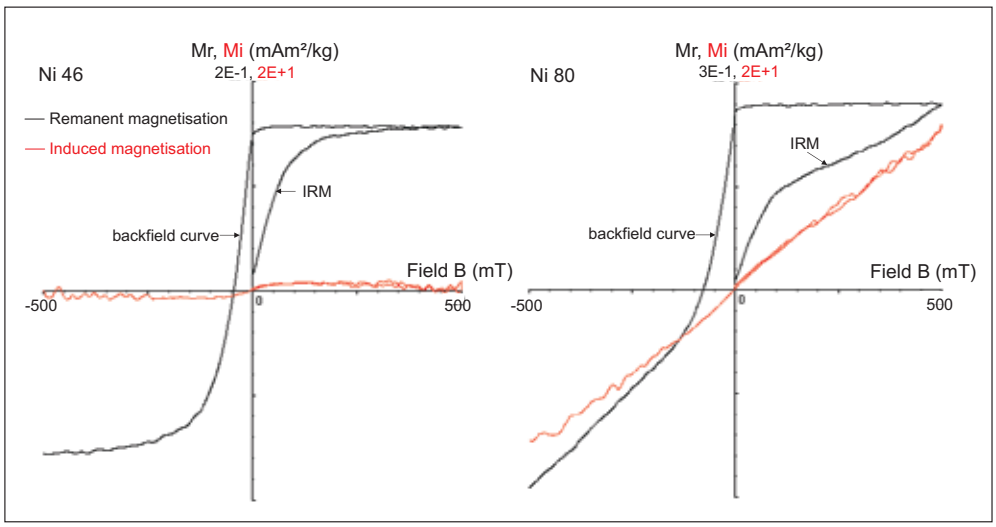

Figure 5. Remanent magnetisation (black) for two samples with different high field IRM contributions. A slight increase between 300 and 500 mT indicates minor hematite contribution in Ni 46 while in Ni 80 hematite contributes much more to the IRM_{500mT} (see text). The hysteresis curves (red) are given for comparison. Note the different scale.

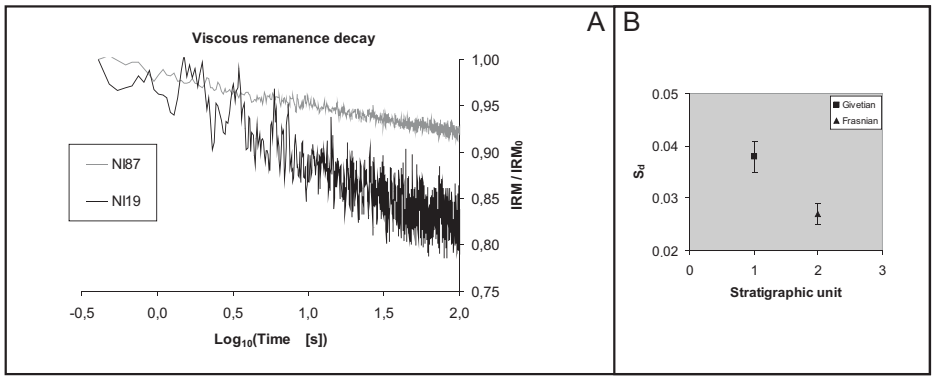

Figure 6. A) The viscous remanence decay of an IRM (500 mT) for two representative samples from the Givetian (Ni19) and the Frasnian (Ni87) observed for 100 s. B) The mean (square or triangle symbols) and the standard deviation values (caps) for the Givetian (13 samples) and Frasnian (3 samples) of the normalized magnetic viscosity coefficient (S_d). Note the difference between the Givetian and Frasnian samples.

Sample number	X_{LF} (m³/kg)	M_s (Am²/kg)	IRM_{500mT} (Am²/kg)	H_c (mT)	H_{cr} (mT)
NI02	7.590E-08	0.001028025	0.000219249	5.66	42.37
NI07	1.64E-08	0.00064163	0.000033172	3.82	38.65
NI09	1.05E-07	0.001293978	0.000119153	4.56	45.13
NI19	2.95E-08	0.001095712	5.72061E-05	3.75	44.70
NI22	5.57E-08	0.001627908	0.000142663	5.16	43.63
NI28	7.72E-08	0.003384058	0.000271713	8.12	49.87
NI34	4.57E-08	0.002139386	0.000199575	10.21	51.36
NI46	5.21E-08	0.002366089	0.000156267	5.67	43.85
NI48	1.44E-08	0.000677239	4.88834E-05	4.72	44.09
NI54	4.64E-08	0.001783794	9.57043E-05	2.95	39.08
NI62	7.50E-08	0.002675498	0.000196301	5.37	47.86
NI63	2.80E-08	0.002282302	6.65584E-05	3.48	47.66
NI75	8.51E-08	0.007680491	0.00019854	6.62	49.49
NI80	9.80E-08	0.016100629	0.000268184	10.01	76.40
NI82	6.97E-08	0.013762907	0.000158593	7.07	51.41
NI87	8.87E-08	0.008145896	0.000267563	8.65	56.33

Sample number	H_{cr}/H_c	X_{HF} (m³/kg)	X_{Ferro} (m³/kg)	S_d	% Hematite contribution
NI02	7.48	3.66487E-09	7.2235E-08	0.034	4.3
NI07	10.12	1.80765E-09	1.4562E-08	0.04	5.2
NI09	9.91	2.23207E-09	1.0257E-07	0.041	5.9
NI19	11.92	1.83222E-09	2.7641E-08	0.073	21.5
NI22	8.46	2.66366E-09	5.3000E-08	0.035	6.3
NI28	6.14	3.4699E-09	7.3730E-08	0.025	7.7
NI34	5.03	2.55072E-09	4.3179E-08	0.023	8.0
NI46	7.73	2.54032E-09	4.9603E-08	0.03	4.5
NI48	9.35	1.46601E-09	1.2977E-08	0.044	13.8
NI54	13.27	3.32754E-09	4.3036E-08	0.042	5.5
NI62	8.92	3.25418E-09	7.1769E-08	0.036	7.0
NI63	13.71	1.62562E-09	2.6408E-08	0.035	11.4
NI75	7.48	2.19903E-09	8.2928E-08	0.032	8.6
NI80	7.63	1.88171E-09	9.6162E-08	0.026	39.3
NI82	7.27	3.7189E-09	6.6021E-08	0.024	10.9
NI87	6.51	2.54637E-09	8.6154E-08	0.03	19.6

Table 1. List of the Nismes samples with the magnetic susceptibility and hysteresis parameters: low-field magnetic susceptibility (X_{LF}), saturation magnetisation (M_s), saturation isothermal remanent magnetisation (IRM_{500mT}), coercive force (H_c), coercivity of the remanence (H_{cr}), magnetisation coercivity ratio (H_{cr}/H_c) , high-field magnetic susceptibility (X_{HF}), ferromagnetic susceptibility (X_{Ferro}), normalized magnetic viscosity coefficient (S_d) and percentage of hematite contribution to the IRM_{500mT}.

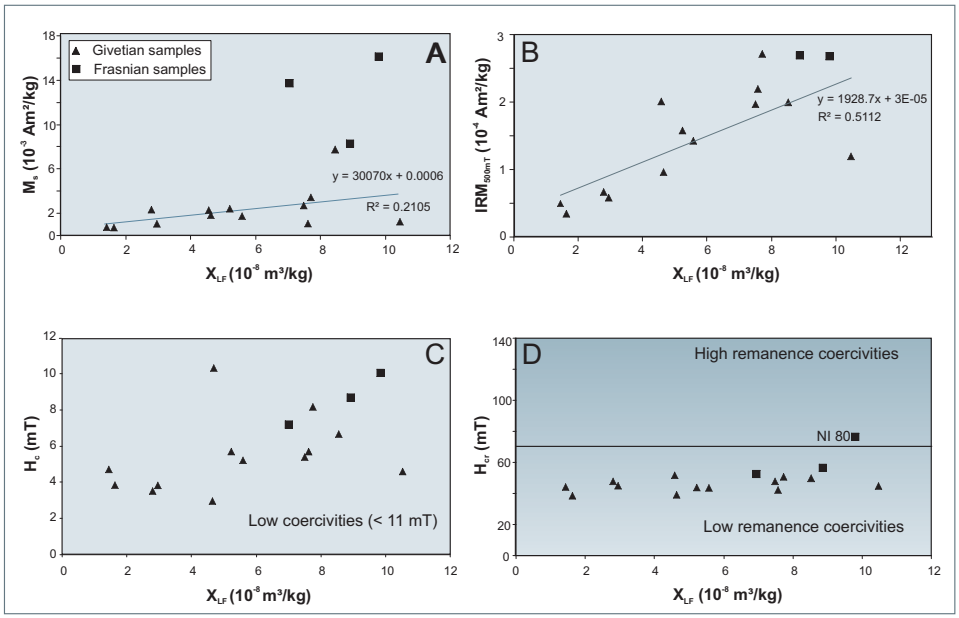

Figure 7. Hysteresis parameters versus X_{LF}. Diagrams: A) saturation magnetisation (M_s) versus X_{LF}, B) saturation isothermal remanent magnetisation at 500 mT (IRM_{500mT}) versus X_{LF}, C) coercive force (H_c) versus X_{LF} and D) coercivity of remanence (H_{cr}) versus X_{LF}. M_s was obtained after correction of the high-field slope to remove the dia- and paramagnetic contributions.

viscous grains, which are generally rather of diagenetic than of detrital origin. The Nismes samples contain thus a non-negligible amount of SP nanoparticles in the ferromagnetic *s.l.* fraction.

The IRM decrease was quantified by the magnetic viscosity coefficient $S_d = \partial M/\partial \lg(t)$, with M being the normalized magnetisation and t the time, which has been calculated for the analysed specimens (Table 1). The normalised magnetic viscosity coefficients are significantly higher in the Givetian than in the Frasnian (Fig. 6B), which may indicate that the Givetian part underwent slightly stronger diagenetic processes forming more SP particles than the Frasnian part. Obvioulsy, there is also a clear correlation with the lithologies as the Givetian is mostly dominated by limestones and the Frasnian is characterized by a higher percentage of detrital rocks. It was also noticed by Zwing et al. (2005), which have provided different normalized magnetic viscosity coefficient for clastic and carbonate rocks.

The M_s values calculated from the hysteresis curve are globally low (between 0.6 and 16 x 10^{-3} Am²/kg) as usually observed for carbonate rocks (Borradaile et al., 1993). M_s data plotted against the X_{LF} (Fig. 7A) show only a weak linear correlation (correlation coefficient R^2 = 0.21) with M_s values ranging between 0.6 and 2.6 x 10^{-3} Am²/kg for the Givetian. The Frasnian samples have very dispersed M_s values, one order of magnitude higher than those reported for the Givetian samples (Fig. 7A). A weak correlation can be observed for the Givetian samples, implying that the MS signal is only partly controlled by the ferromagnetic contributions. However, Riquier et al. (in press) has reported much stronger correlation coefficients in Frasnian-Famennian sections in Europe. The diagram reporting the IRM_{500mT} values in front of X_{LF} (Fig. 7B) show globally a better correlation (R^2 = 0.51). Remanence magnetisation at saturation correlated with magnetic susceptibility is also an indication of the ferromagnetic contribution to the MS signal..

The nature of the ferromagnetic *s.l.* fraction has been investigated using measurements of the coercive force H_c and the coercivity of the remanence H_{cr} (Table 1). The magnetic mineralogy is dominated by low coercive minerals in all samples (Fig. 7C). Consequently, also the remanence coercive forces are low (< 70 mT) regardless X_{LF} for most of the samples (Fig. 7D). H_{cr} values ranging between 8 and 69.5 mT correspond to magnetite mineral

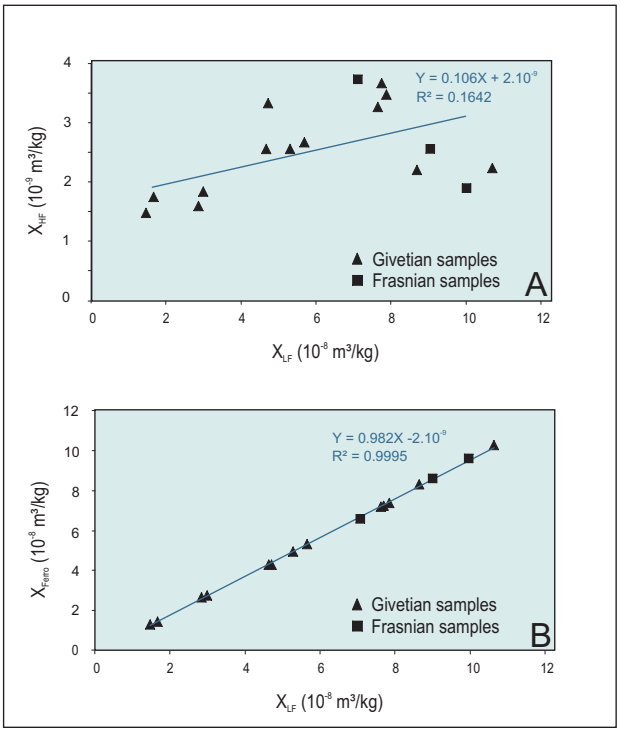

Figure 8. A) The high-field magnetic susceptibility (X_{HF}) reported versus the low-field magnetic susceptibility (X_{LF}) shows only a broad positive correlation (R^2 = 0.16). B) The ferromagnetic susceptibility (X_{Ferro}) reported versus the low-field magnetic susceptibility (X_{LF}) is characterized by a strong positive linear correlation (R^2 = 0.99).

based on a compilation of data of synthetic and natural samples (Peters & Dekkers, 2003). Even in the same range of coercivity values (< 70 mT), the Frasnian samples have faintly higher average coercivity values (58.4 mT) compared to the Givetian ones (44.9 mT). Only one Frasnian sample (Ni 80) has a slightly higher H_{cr} value of 76.4 mT. However, as the backfield curve shows clearly contribution of low and high coercive minerals, the measured H_{cr} values (including the one of 76.4 mT) are rather caused by a mixture of two magnetic mineral populations with low and high remanent coercive forces and may not correspond to a single magnetic phase. As there is also no evidence of pyrrhotite from thermomagnetic measurements (see Fig. 4), its presence is practically excluded.

The X_{HF} values are generally very low (below 4.0 x 10^{-9} m³/kg) with a very weak linear correlation ($R^2 = 0.16$) between X_{HF} and X_{LF} (Fig. 8A, Table 1). This indicates a minor contribution of the matrix components to the low-field magnetic susceptibility. A strongly significant linear correlation ($R^2 = 0.99$) between X_{Ferro} and X_{LF} is seen even if the concentration of the ferromagnetic minerals is weak; as a consequence these minerals probably control most of the MS signal fluctuations (Fig. 8B, Table 1).

5. Discussion

5.1. Magnetic mimerals carrying the MS signal

Hysteresis parameters reveal: (1) low H_c (< 12 mT) and H_{cr} values (< 70 mT) regardless of the X_{LF} values for most of the samples indicating the presence of a low coercivity mineral of magnetite type phase; (2) a strong linear correlation between the ferromagnetic susceptibility and the low-field magnetic susceptibility suggesting that even if the concentration in ferromagnetic minerals is weak, they probably control most of the MS signal fluctuations; (3) the participation to the MS signal of diamagnetic and paramagnetic (mainly iron-bearing clay minerals and pyrite) fractions and their probable increase upsection.

The M_{rs} / M_s and B_{cr} / B_c ratios of the gray/white Maiolica limestone (Jurassic of Italy) are respectively generally high (above 0.1) and moderately low (between 1.5 and 5). Primary MD magnetite and SD biogenic magnetite are suggested for these unremagnetised limestones (Channel & McCabe, 1994). These authors have also reported an increase in the proportion of detrital MD magnetite upsection concomitant with an increase of the paramagnetic minerals related to increasing detrital clay content. Increasing detrital clay content is evident upsection in Nismes as indicated by the abrupt lithological changes at the Givetian-Frasnian boundary. Our data differ clearly with the pink/red Jurassic limestones (Scaglia, Ammonitico Rosso and Corniola) of Italy that have M_{rs} / M_s ratios generally high (above 0.1) and moderately higher B_{cr} / B_c ratios ($2 < B_{cr} / B_c < 20$). These remagnetised limestones have magnetite and hematite contributions to the remanence with hematite produced during diagenesis (Channel & McCabe, 1994). The coercivity ratios (Table 1) measured in the Nismes section range between 5.03 and 13.71. The magnetisation ratios cannot be directly used due to the presence of a mixture of magnetite and hematite grains in the ferromagnetic s.l. fraction. Nevertheless, there isn't any evidence of red pigmentation in the Givetian limestones nor in the shales to suggest a similar origin and diagenetic evolution at the Givetian-Frasnian boundary of the Nismes section. The grain sizes of the different magnetite population grains could not be inferred from the Day plot as the magnetisation ratios are probably underestimated due to the hematite grains.

In their study on the remagnetised Devonian limestones (essentially of Givetian age) of the Ardennes-Boulonnais area, Zegers et al. (2003) presented hysteresis properties consistent with a mixture of magnetite grains corresponding to large SP grains with a relatively small proportion of grains in the SD range (NRM component C) and pyrrhotite acquiring the NRM component P. The Boulonnais area is clearly identified in the hysteresis properties with lower magnetisation and coercivity ratios close to the trend of the unremagnetised Maiolica limestones as defined by Channel & McCabe (1994). These magnetite grains from the Boulonnais straddle the SD-MD mixing line derived on theoretical grounds by Dunlop (2002) and are therefore interpreted as primary preserved detrital magnetite. It could be also suggested from the hysteresis data that part of the magnetite (i.e. the coarse grained grains) in the Nismes section are primary detrital magnetite.

Fig. 9 summarises the results of the detailed rock magnetic analyses. Apart from fluctuations, one sees a slight increasing trend of X_{Ferro} and IRM_{500mT} from the Givetian to the Frasnian. This is related to grain sizes and/or concentration changes of magnetic minerals. The saturation magnetisation varies similarly as X_{Ferro} and IRM_{500mT} but shows a more pronounced increase in the Frasnian. Because M_s depends only on concentration and not on grain size, it reflects only the ferrimagnetic mineral fraction, *i.e.* a magnetite type phase and hematite in our case. The viscous decay (S_d) shows rather opposite trends to M_s, IRM_{500mT} and X_{Ferro}, which indicates that the enhancement of ferrimagnetic minerals is not caused by SP grains. However, small but significant amounts of SP grains seem to be present, particularly in the Givetian. Their presence indicates that diagenetic processes have occurred involving neoformation of small amounts of ferromagnetic nanoparticles.

Bacteria are producing SP magnetite or maghemite nanoparticles in oxygen-depleted microenvironments in the carbonate laminated mats of the Holocene carbonate peritidal muds deposited in the Triple Goose Creek region of Andros Island (Bahamas) (Maloof et al., 2007). These environments are observed in cores from the Bahamas isolated carbonate platform where the clastic input is reduced. The stronger magnetic part was found in the laminated intertidal to supratidal beds of shoaling-upward meter-scale parasequences and are related to syn-depositional cementation process (Maloof et al., 2007). Other occurrences of these microbially precipitated and/or mediated magnetites were found in microborings in

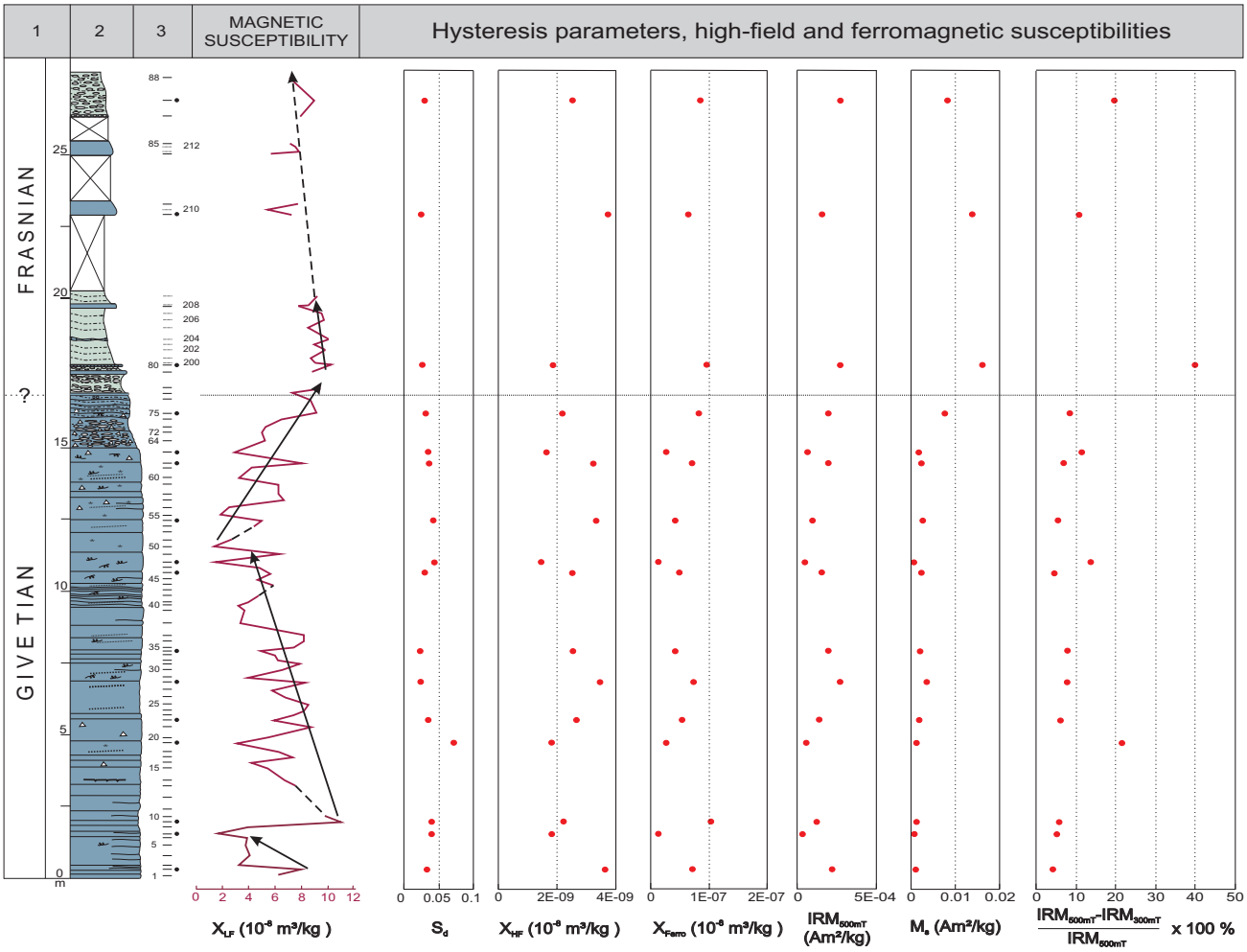

Figure 9. Detailed rock magnetic analyses plotted along the lithological column. From left to right: (1) stratigraphy, (2) lithological column, (3) position of the samples, low-field magnetic susceptibility (X_{LF}), normalized magnetic viscosity coefficient (S_d), high-field magnetic susceptibility X_{HF}, ferromagnetic susceptibility X_{Ferro}, saturation isothermal remanent magnetisation at 500 mT (IRM_{500mT}), saturation magnetisation (M_s), and percentage of hematite contribution to the IRM_{500mT}. Note the higher values of IRM_{500mT}, M_s and the higher percentage of hematite contribution to the IRM_{500mT} for the Frasnian.

oolite banks, allochems and cements (Hladil et al., 2004). The preservation of ancient bacterial SP magnetite grains until present days is still a matter of debate as often-anoxic conditions occur during post-depositional diagenesis (pers. com. Mark Dekkers). The fluctuation of the percentage of SP magnetite in the Nismes section as revealed by the viscous decay are not correlated with the microfacies indicating probably another origin of these nanoparticles. A large amount of SP magnetite is observed in the Mraznica Formation of Slovakia at the Jurassic-Cretaceous boundary. A chemical remagnetisation model is proposed by Grabowski et al. (2009) implying the circulations of oxidizing fluids and the precipitation of new magnetite by oxidation of pyrite. This chemical remagnetisation process seems to be not valid in the Nismes section as high amounts of fine-grained pyrite (5-10 µm), pyritospheres and filamentous pyrite have been described in the matrix of most of the microfacies by Casier & Préat (2009). The formation of nanomagnetites could be also related to the chemical reaction of smectite to illite conversion reaction during burial diagenesis (Katz et al., 1998, 2000) and is argued by Zegers et al. (2003) as the main mechanism to explain the presence of a mixture of SP-SD magnetite (component C) in the dark grey Givetian limestones of the Ardennes. However, the Nismes section seems to contain a lesser amount of SP magnetite compared to the results of the remagnetised Givetian samples where a large contribution of 8-10 nm grains is inferred from the Day Plot in Zegers et al. (2003). The origin and the nature of the superparamagnetic particles identified here cannot easily be determined without additional analyses like Mössbauer spectroscopy (MBS) on magnetic extracts or heavy liquid separates.

The percentage of hematite contribution to the IRM_{500mT}, as already described in § 4.2., increases from the Givetian to the Frasnian, if one neglects the values of the sample Ni 19 and Ni 80 (Fig. 9 and Table 1). Detrital illite and kaolinite are the essential minerals determined by XRD in poorly consolidated mudstones of the Abo Formation (Permian of New Mexico, USA), which contain hematite disseminated throughout the matrix and also as coatings on detrital grains (Bensing et al., 2005). Illite contains iron as a primary constituent in the crystal structure and kaolinite could transport iron on crystal

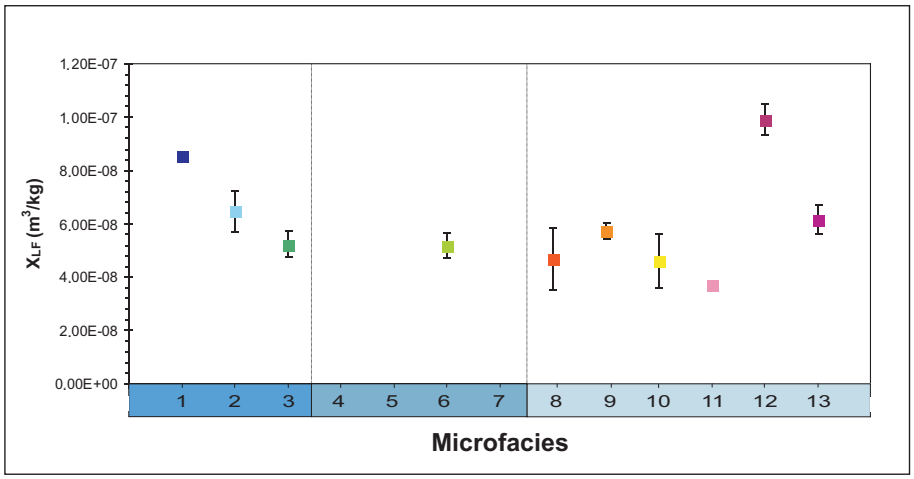

Figure 10. The mean X_{LF} (square symbol) and the standard deviation (caps) values for the 10 recognised microfacies of the Nismes section. X_{LF} values decrease in the open-marine microfacies from MF1 to MF3. The X_{LF} values increase in the open-marine peri-reefal environments and show large fluctuations in the restricted environments with lowest and highest MS values respectively for microfacies MF11 and MF12.

surfaces as ferric oxyhydroxides and these iron oxyhydroxide precursors were subsequently altered to hematite at low temperature (< 85°C) during shallow burial (Bensing et al., 2005). Lithologies in the Nismes section and the microfacies analysis do not reveal any reddening of the rocks suggesting a similar diagenetic origin of the hematite. It is therefore suggested that hematite is only present in limited amount in the rocks at the Givetian-Frasnian boundary. Because the hematite IRM contributions do not correlate with the viscous decay, hematite is here interpreted to be of detrital origin with a higher abundance in the Frasnian. Other magnetic minerals than magnetite carrying the remanence in the studied limestones and/or shales like hematite are evident and need to be further examined with other techniques.

The paramagnetic contribution is certainly linked with the presence and increasing abundance upsection of clay minerals and pyrite (?). Detailed clay mineralogy and eventual fluctuations of the clay-mineral assemblage need to be further analyzed. Fine-grained (5-10 µm) to coarse-grained (100-300 µm) pyrite grains and abundant pyritospheres have been observed during petrographic analysis in the matrix, in the bioclasts or in the microstylolites in most of the microfacies (Casier & Préat, 2009). The fine-grained pyrite grains are observed in open-marine and restricted environments while peri-reefal environments show coarse-grained pyritic grains. A detrital origin for the pyrite content is improbable because pyrite is physically and chemically unstable during typical conditions of transport and deposition (Berner, 1984). It remains unclear whether the source material for its formation is of detrital origin or formed *in situ* by bacterial productivity. The ferromagnetic and paramagnetic grain populations are partly of detrital origin and control the fluctuations of the MS signal in the Nismes section.

5.2. Comparison between microfacies and MS curves

As reported on Fig. 2, the correlations between MS and microfacies curves are very weak. MS fluctuations and microfacies evolutions are generally not correlated at the base of the section and anti-correlated in the middle part of the studied section as indicated by the opposite evolutions of the shallowing-upward sequences 3-4, the slight deepening-upward sequence 5 and the magnetic sequences 2 and 3. A pattern with good parallel concordance of both curves is only observed during the transgressive trend from restricted supratidal lagoon environment (MF12-13) at the end of the microfacies sequence 1 passing progressively to open-marine setting (MF2-3) at the top of the microfacies sequence 3. This trend is also observed in the MS curve by decreasing MS values from 7.02 to 3.22 x 10^{-8} m³/kg. This evolution corresponds partially to the magnetic sequences 2. In details, MS and microfacies do not reveal a similar or concordant evolution along the lithostratigraphic column.

By plotting the mean MS value with their standard deviation for each microfacies against the microfacies standard sequence (MF1-13) of the Givetian carbonate platform, there isn't any clear linear correlation (Fig. 10). The mean MS value decreases from 8.51 x 10^{-8} m³/kg for the microfacies MF1 to 5.25 x 10^{-8} m³/kg for the microfacies MF3 in the open-marine environment under the influence of storm activities along a distal to proximal gradient (MF1-3). This decreasing evolution of the mean MS values in the Nismes section is also observed in the first deepest environments of the Frasnian (Da Silva et al., 2009) and Eifelian-Givetian platforms of Belgium (Mabille & Boulvain, 2008; Da Silva et al., 2009). The average MS value (5.73 x 10^{-8} m³/kg) for the microfacies 9 is a little higher than the one of the microfacies 3. The evolution is relatively stable in peri-reefal environment and does not reveal any large MS change due to the absence of high energetic barrier environments (MF4, MF5 and MF7) at the end of the Fromelennes Formation. The mean MS values remain more or less stable in the restricted intertidal to supratidal lagoonal environments. The highest mean MS value (9.90 x 10^{-8} m³/kg) corresponds to the supratidal microfacies MF12 close to the emersion. Lower mean MS value (6.14 x 10^{-8} m³/kg) is then observed in the semi-evaporitic fine-grained dolomudstones environment. This evolution in the restricted lagoonal environment is also relatively similar with those described for the Frasnian and Eifelian-Givetian platforms (Da Silva et al., 2009). These authors report the highest mean MS

values (8.6 and 9.3 x 10^{-8} m^3/kg) respectively for the supratidal lagoonal facies a6 of the Frasnian platform and for the lagoonal facies b7 of the Eifelian-Givetian platform. Both values are lower compared to the one of the microfacies MF12 of the Nismes section.

According to Da Silva et al. (2009), on carbonate platforms, average MS generally increases towards the top of shallowing-upward sequences and the average MS along a distal-proximal profile shows intermediate values in the deepest facies, decreases for the reef belt and increases to a maximum in the shallowest facies (back reef zone). MS and microfacies curves have thus a mimetic trend on carbonate platforms, which is not the case on carbonate ramp and atolls. In ramps and atolls, the average MS generally decreases towards the top of shallowing-upward sequences and the average MS along a distal-proximal profile shows the highest values in the outer ramp, decreases towards the lowest values in the middle ramp and increases slightly in the inner ramp. In these two cases, MS and MF curves are anti correlated and are characterized by opposite trends. The MS curve and the average MS profile of the Nismes section show several discrepancies with the models presented for the carbonate platforms and for the carbonate ramp and atolls by Da Silva et al. (2009) indicating here an intermediate behaviour.

A link between microfacies evolutions or sea-level fluctuations and MS changes is not necessarily evident taking into account the previous sedimentological parameters and the different possible sources of the magnetic minerals. MS fluctuations recorded in sedimentary series could also be influenced: by changes in the concentration of (1) different ferromagnetic grain populations such as the goethite and hematite concentrations variations in the paleosols and loess sequences of China (Balsam et al., 2004) or (2) different paramagnetic grain populations such as the illite/chlorite ratio in a fine-grained siliciclastic sequence of the Late Llandovery (English, 1999), by changes in the grain size of the magnetic minerals (Maher, 1988; Chen et al., 2005), by the transformation of primary grains into secondary magnetic minerals during diagenesis (Katz et al., 2000; Chen et al., 2005) and by tectonic activity and/or fluid circulations (Zegers et al., 2005). These assertions imply the need of detailed analyses on the magnetic mineralogy to identify clearly the magnetic carriers of the signal, their grain sizes and to determine the primary or secondary origin of these minerals.

Nevertheless the opposite evolutions of the microfacies sequence 5 and the magnetic sequence MSE 3 could thus be interpreted in terms of detrital changes indicated by the ferromagnetic and paramagnetic contributions. The transition at the Givetian/Frasnian boundary from a carbonate platform (Fromelennes Formation) to a siliciclastic ramp (Nismes Formation) corresponds to the drowning event of the carbonate platform and should correspond to the end of a final highstand system tract (HST). The position of the drowning unconformity related to the sea-level rise could correspond precisely to the position of the SL3 reported in Casier & Préat (2009) as indicated by an abrupt changes from semi-restricted subtidal lagoon to open-marine environment at the end of the Fort Hulobiet Member. The latter shows an opening of the carbonate platform, attested by a faunal diversification, announcing the large marine transgression at the base of the Frasnian (Boulvain et al., 2009). The microfacies sequences 1, 2 and 3+4 consist of meter-scale cycles recording three successive slight shallowing-upward evolutions separated by sea-level rises indicating the progressive deepening of the platform. This change is accompanied by a progressive increase of detrital terrigenous clastic sediment from the continental sources to the marine realm. The progressive increase of the X_{LF} values during the MSE 3 could record this event, starting at the base of this magnetic sequence. The microfacies sequence 5 stays in the open-marine environment, under the influence of storm activities, and records a small deepening of the environment near the top of the sequence as indicated by the transition from packstones to mudstones. The facies are not changing drastically during this last microfacies sequence but the progressive input of detrital ferromagnetic minerals is clearly recorded by the evolution of the MS signal. It is therefore suggested that the MS signal records undoubtedly a slight and progressive modification of the detrital content related to the arrival of coarser ferromagnetic minerals (i.e. magnetite type phase and hematite). This evolution is observed by the MS signal with a higher precision compared to the microfacies. Anyway the transition from the microfacies sequence 4 to 5 records a clear and strong sea-level rise, which probably corresponds to the real modification of the paleoenvironments. This multidisciplinary study could reinforce the difference between stratigraphical limits fixed on the base of lithological changes and the onset of the drowning of the Givetian carbonate platform identified by means of microfacies and MS several beds before. The lithological sharp contact between the end of the Fort Hulobiet Member (Fromelennes Formation) and the 40 metres thick Nismes Formation is relatively constant in all the sedimentation area (Boulvain et al., 2009).

6. Conclusions

In the Nismes section the susceptibility is consistently positive, which means that the carbonates contain impurities of ferromagnetic and paramagnetic minerals. The rock magnetic analyses give evidence that the fluctuations in the MS signal throughout the sections are caused by concentration changes of the detrital ferromagnetic fraction. It evolves upsection from a mixture of fine-grained authigenic SP and coarser-grained detrital magnetite associated to hematite in the Givetian to the progressive contribution of hematite and more coarse-grained magnetite and a smaller contribution of nanoparticles to the MS signal in the Frasnian. IRM curves indicate the presence of a high coercivity mineral phase, which corresponds probably to hematite grains. It is proposed that partly magnetite and hematite population grains are of detrital origin. Different grain sizes magnetite

type phase, hematite, clay minerals and pyrite are participating to the MS signal and it is argued that the ferromagnetic minerals are controlling the MS signal as indicated by the strong correlation between ferromagnetic and low-field susceptibilities. The concentration of ferromagnetic minerals is increasing in the Frasnian and the hematite contributions are progressively increasing from the Givetian to the Frasnian.

The recognised microfacies are described from open-marine environments under the influence of storms to restricted environments with semi-evaporitic conditions. The microfacies curve reveals three shallowing-upward parasequences separated by sea level rises. Gradual transgressions are observed and have affected the carbonate platform during three pulses, the last one leaves the peri-reefal and restricted environments for the deepest open-marine environments. The shallower part of the carbonate platform, corresponding to the restricted lagoon and peri-reefal environments (microfacies MF13 to MF4), shows a small decrease of the mean X_{LF} values along a proximal to distal transect interrupted by a strong increase of the mean X_{LF} values for the mudstones of the microfacies MF12. The open-marine environment under the influence of storm activities, represented essentially by the microfacies MF1 to MF3 in the sequence 5, presents a positive gradient towards higher mean X_{LF} values in the distal part of the platform as indicated also by the magnetic sequence MSE 3. These fluctuations along the platform profile could be partially controlled by the decreasing influence of hydrodynamic (wave agitation) energy of the environment, the carbonate production and the sedimentation rate among other parameters (Da Silva et al., 2009). The MS profile presented here has an intermediate behaviour between carbonate platform and ramp environments corresponding to the transitional step during the drowning of the Givetian platform and the onset of the Frasnian ramp. These opposite evolutions of the microfacies and MS curves are concomitant with a major sea level rise and correspond to the drowning of the Givetian carbonate platform and the final HST. The drowning is associated to an increased terrigenous influx leading to higher X_{LF} values during the lower part of the Nismes Formation in the Frasnian. Both microfacies and rock magnetism highlight the change and progressive influx of more detrital minerals to the marine realm in relation with the drowning of the Givetian carbonate platform, which seems to be several beds below the lithostratigraphical changes and the Givetian-Frasnian boundary.

7. Acknowledgements

The second author thanks the Belgian Science Policy for funding the research program “Rock magnetism and sedimentology of the Givetian”. This study is a contribution to the IGCP 580 project entitled “Application of magnetic susceptibility on Paleozoic sedimentary rocks”. The authors thank A.-C. Da Silva and F. Boulvain for managing a special edition of Geologica Belgica dedicated to MS application in sedimentary series for which this paper is a contribution. The final version of the manuscript was considerably improved by the reviews of M. Dekkers and J. Hladil. The third author acknowledges financial support via project “Vallée Magnétique” endorsed by the Belgian Minister of Small and Medium-sized Enterprises, Self-employment, Agriculture and Scientific Research Mrs S. Laruelle, and the Secretary of State for Social Affairs in charge of Disabled People, Mr J.-M. Delizée.

8. References

BALSAM, W., JUNFENG, J. & CHEN, J., 2004. Climatic interpretation of the Luochan and Lingtai loess sections, China, based on changing iron oxide mineralogy and magnetic susceptibility. *Earth and Planetary Science Letters*, 223: 335-348.

BENSING., J.P., MOZLEY, P.S. & DUNBAR, N.W., 2005. Importance of clay in iron transport and sediment reddening: evidence from reduction features of the Abo Formation, New Mexico, USA. *Journal of Sedimentary research*, 75: 562-571.

BERNER, R.A., 1969. Goethite stability and the origin of red beds. *Geochemica et Cosmochemica Acta*, 33: 267-273.

BERNER, R.A., 1984. Sedimentary pyrite formation: an update. *Geochemica et Cosmochemica Acta*, 48: 605-615.

BLOEMENDAL, J., KING, J.W., TAUXE, L. & VALET, J.-P., 1989. Rock magnetic stratigraphy of Leg 108 Sites 658, 659, 661 and 665, eastern tropical Atlantic. *In* Ruddiman, W.F. et al. (eds), *Proceedings of the Ocean Drilling Program, Initial Reports,* 108 (College Station, TX): 415-428.

BORRADAILE, G.J., CHOW, N. & WERNER, T., 1993. Magnetic hysteresis of limestones: facies control? *Physics of the Earth and Planetary Interiors*, 76: 241-252.

BORRADAILE, G.J. & LAGROIX, F., 2000. Magnetic characterization using a three-dimensional hysteresis projection, illustrated with a study of limestones. *Geophysical Journal International*, 141: 213-226.

BOULVAIN , F., BULTYNCK, P., COEN, M., COEN-AUBERT, M., LACROIX, D., LALOUX, M., CASIER, J.-G., DEJONGHE, L., DUMOULIN, V., GHYSEL, P., GODEFROID, J., HELSEN, S., MOURAVIEFF, N., SARTENAER, P., TOURNEUR, F. & VANGUESTAINE, M., 1999. Les Formations du Frasnien de la Belgique. *Memoirs of the Geological Survey of Belgium,* 44: 1-126.

BOULVAIN, F., DA SILVA, A.-C., MABILLE, C., HLADIL, J., GERSL, M., KOPTIKOVA, L. & SCHNABL, P., 2010. Magnetic susceptibility correlation of km-thick Eifelian-Frasnian sections (Ardennes and Moravia). *Geologica Belgica*, this volume.

BOULVAIN, F., MABILLE, C., POULAIN, G. & DA SILVA, A.-C., 2009. Towards a palaeogeographical and sequential framework for the Givetian of Belgium. *Geologica Belgica*, 12: 161-178.

BULTYNCK, P., 1987. Pelagic and neritic conodont successions from the Givetian of pre-Sahara Morocco and the Ardennes. *Bulletin de l'Institut royal des Sciences naturelles de Belgique, Sciences de la Terre*, 57: 149-181.

BULTYNCK, P., CASIER, J.-G., COEN, M., COEN-AUBERT, M., GODEFROID, J., JACOBS, L., LOBOZIAK, S., SARTENAER, P. & STREEL, M., 1988a. Pre-Congress excursion to the Devonian stratotypes in Belgium. *Bulletin de la Société belge de Géologie,* 95(3): 249-288.

BULTYNCK , P., DREESEN, R., GROESSENS, E., STRUVE, W., WEDDIGE, K., WERNER, R. & ZIEGLER, W., 1988b. Field Trip A (22-24 July, 1988), Ardennes (Belgium) and Eifel Hills (Federal Republic of Germany). *Courier Forschunginstitut Senckenberg,* 102: 7-85.

BUROV, B., NURGALIEV, D.K. & JASONOV, P.G., 1986. Paleomagnetic Analysis. Kazan University Press (in Russian): 176 pp.

CASIER, J-G. & PRÉAT, A., 2007. Ostracods and lithofacies of the Middle/Upper Devonian boundary stratotype (Puech de la Suque, Montagne Noire, France). *Bulletin de la Société géologique de France*, 4: 293-304.

CASIER, J-G. & PRÉAT, A., 2009. Late Givetian to Middle Frasnian ostracods from Nismes (Dinant Synclinorium, Belgium) and their lithological context. *Bulletin de l'Institut royal des Sciences naturelles de Belgique, Sciences de la Terre*, 79: 87-115.

CASIER, J-G., CAMBIER, G., DEVLEESCHOUWER, X., PETITCLERC, E. & PRÉAT, A., 2009. Ostracods, rock facies and magnetic susceptibility of the Trois-Fontaines/Terres d'Haurs transition in the type locality for the Givetian. *GSA Annual Meeting, Portland, USA, 18-21 October 2009, Abstracts with Programs*, 41(7): 107.

CHANNELL, J.E.T. & MCCABE, C., 1994. Comparison of magnetic hysteresis parameters of unremagnetized and remagnetized limestones. *Journal of Geophysical Research*, 99: 4613-4623.

CHEN, T., HUIFANG, X., XIE, Q., CHEN, J., JI, J. & LU, H., 2005. Characteristics and genesis of maghemite in Chinese loess and paleosols: mechanism for magnetic susceptibility enhancement in paleosols. *Earth and Planetary Science Letters*, 240: 790-802.

CHRISTENSEN, A.N., JENSEN, T.R., BAHL, C.R.H. &

DIMASI, E., 2007. Nano size crystals of goethite, □-FeOOH: Synthesis and thermal transformation. *Journal of Solid State Chemistry*, 180: 1431–1435.

CRICK, R.E., ELLWOOD, B. & El HASSANI, A., 1994. Integration of biostratigraphy, magnetic susceptibility and relative sea-level change: a new look at high resolution correlation. *Subcommission on Devonian Stratigraphy, Newsletter*, 11: 59-66.

CRICK, R.E., ELLWOOD, B., El HASSANI, A. & FEIST, R., 2000. Proposed magnetostratigraphy susceptibility magnetostratotype for the Eifelian-Givetian GSSP (Anti-Atlas, Morocco). *Episodes*, 23(2): 93-101.

CRICK, R.E., ELLWOOD, B., El HASSANI, A., FEIST, R. & HLADIL, J., 1997. MagnetoSusceptibility Event and Cyclostratigraphy (MSEC) of the Eifelian-Givetian GSSP and associate boundary sequences in North Africa and Europe. *Episodes*, 20(3): 167-175.

CRICK, R.E., ELLWOOD, B.B., HLADIL, J., EL HASSANI, A., HROUDA, F. & CHLUPAC, I., 2001. Magnetostratigraphy susceptibility of the Pridolian-Lochkovian (Silurian-Devonian) GSSP (Klonk, Czech Republic) and coeval sequence in Anti-Atlas Morocco. *Palaeogeography, Palaeoclimatology, Palaeoecology*, 167: 73-100.

DA SILVA, A.-C., MABILLE, C. & BOULVAIN, F., 2009. Influence of sedimentary setting on the use of magnetic susceptibility : examples from the Devonian of Belgium. *Sedimentology*, 56: 1292-1306.

DEVLEESCHOUWER, X., 1999. *La limite Frasnien-Famennien (Dévonien Supérieur) en Europe: sédimentologie, stratigraphie séquentielle et susceptibilité magnétique*. Thèse de Doctorat en Sciences géologiques et minéralogiques, Université Libre de Bruxelles et Université des Sciences et Technologies de Lille, 414 p. [In French, with English abstract ; unpublished].

DEVLEESCHOUWER, X., PRÉAT, A., AVERBUCH, A. & HERBOSCH, A. 1999. *Magnetic susceptibility through the Frasnian-Famennian boundary (Steinbruch Schmidt, Germany and Coumiac, France)*. 19th regional European Meeting of Sedimentology, Copenhagen, Denmark, Abstract book: 71-72.

DEVLEESCHOUWER, X., CAMBIER, G., PETITCLERC, E., CASIER, J-G. & PRÉAT, A., 2009. *Givetian platform carbonates (Givet, France): rock magnetism, microfacies interpretation and ostracods study*. 12e Colloque de l'ASF, Rennes, France, 25-31 October 2009, 107.

DUNLOP, D.J., 2002. Theory and applications of the Day Plot (Mrs/Ms versus Hcr/Hc): 1. Theoretical curves and tests using titanomagnetite data. *Journal of Geophysiscal Research*, 107(B3), doi: 10.1029/ 2001JB000486.

DUNLOP, D.J. & ÖZDEMIR, Ö., 1997. *Rock magnetism. Fundamentals and frontiers*. Cambridge University Press: 573 pp.

ELLWOOD, B., BENOIST, S.L., EL HASSANI, A., WHEELER, C. & CRICK, R.E., 2003. Impact ejecta layer from the Mid-Devonian: possible connection to global mass extinctions. *Science*, 300 (5626), 1734-1737.

ELLWOOD, B., BRETT, C.E. & MACDONALD, W.D., 2007. Magnetostratigraphy susceptibility of the Upper Ordovician Kope Formation, northern Kentucky. *Palaeogeography, Palaeoclimatology, Palaeoecology*, 243: 42-54.

ELLWOOD, B., CRICK, R.E. & EL HASSANI, A., 1999. The Magneto-Susceptibility Event and Cyclostratigraphy (MSEC) method used in geological correlation of Devonian rocks from Anti-Atlas Morocco. *American Association of Petroleum Geology Bulletin*, 83(7): 1119-1134.

ELLWOOD, B., CRICK, R.E., EL HASSANI, A., BENOIST, S.L. & YOUNG, R.H., 2000. Magnetosusceptibility event and cyclostratigraphy method applied to marine rocks: detrital input versus carbonate productivity. *Geology*, 28(12): 1135-1138.

ELLWOOD, B., CRICK, R.E., GARCIA-ALCADE FERNANDEZ, J.L., SOTO, F.M., TRUYOLS-MASSONI, M., EL HASSANI, A. & KOVAS, E.J., 2001. Global correlation using magnetic susceptibility data from Lower Devonian rocks. *Geology*, 29(7): 583-586.

ELLWOOD, B., TOMKIN, J.H., RATCLIFFE, K.T., WRIGHT, M. & KAFAFY, A.M., 2008. High-resolution magnetic susceptibility and geochemistry for the Cenomannian/Turonian boundary GSSP with correlation to time equivalent core. *Palaeogeography, Palaeoclimatology, Palaeoecology*, 261: 105-126.

ENGLISH, L.T.P., 1999. The use of magnetic susceptibility and trace element geochemistry for the correlation of fine-grained siliciclastic sequences: a Late Llandovery example from northwest England. *Geological Magazine*, 136(4): 423-436.

EVANS, M.E. & HELLER, F., 2003. *Environmental magnetism. Principles and Applications of enviromagnetics*. Academic Press, Elsevier Science: 299 p.

FIELITZ, W. & MANSY, J.-L., 1999. Pre- and synorogenic burial metamorphism in the Ardenne and neighbouring areas (Rhenohercynian zone, central European Variscides). *Tectonophysics*, 309: 227-256.

GORBARENKO, S.A., NÜRNBERG, D., DERKACHEV, A.N., ASTAKHOV, A.S., SOUTHON, J.R. & KAISER, A., 2002. Magnetostratigraphy and tephrochronology of the Upper Quaternary sediments in the Okhotsk Sea: implication of terrigenous, volcanogenic and biogenic matter supply. *Marine Geology*, 183: 107-129.

GRABOWSKI, J., MICHALIK, J., SZANIAWSKI, R. & GROTEK, I., 2009. Synthrusting remagnetization of the Krizna nappe: high-resolution palaeo- and rock magnetic study in the Strazovce section, Strazovske vrchy Mts, Central West Carpathians (Slovakia). *Acta Geologica Polonica*, 59(2): 137-155.

HELSEN, S., 1992. Conodont colour alteration maps for Paleozoic strata in Belgium, northern France and westernmost Germany – preliminary results. *Annales de la Société Géologique de Belgique*, 115: 135-143.

HLADIL, J., 2002. Geophysical records of dispersed weathering products on the Frasnian carbonate platform and early Famennian ramps in Moravia, Czech Republic: proxies for eustasy and paleoclimate. *Palaeogeography, Palaeoclimatology, Palaeoecology*, 181: 213-250.

HLADIL, J., CAREW, J.L., MYLROIE, J.E., PRUNER, P., KOHOUT, T., JELL, J.S., LACKA, B. & LANGROVA, A., 2004. Anomalous magnetic susceptibility values and traces of subsurface microbial activity in carbonate banks on San Salvador Island, Bahamas. *Facies*, 50: 161-182.

HLADIL, J., CEJCHAN, P., BABEK, O., KOPTIKOVA, L., NAVRATIL, T. & KUBINOVA, P., 2010. Dust –A geology-orientated attempt to reappraise the natural components, amounts, inputs to sediment, and importance for correlation purposes. *Geologica Belgica*, this volume.

HLADIL, J., GERSL, M., STRNAD, L., FRANA, J., LANGROVA, A. & SPISIAK, J., 2006. Stratigraphic variation of complex impurities in platform limestones and possible significance of atmospheric dust: a study with emphasis on gamma-ray spectrometry and magnetic susceptibility outcrop logging (Eifelian-Frasnian, Moravia, Czech Republic). *International Journal of Earth Sciences*, 95: 703-723.

HROUDA, F., 1994. A technique for the measurement of thermal changes of magnetic susceptibility of weakly magnetic rocks by the CS-2 apparatus and KLY-2 Kappabridge. *Geophysical Journal International*, 118: 604-612.

KATZ, B., ELMORE, D.R., COGOINI, M. & FERRY, S., 1998. Widespread chemical remagnetization: orogenic fluids or burial diagenesis of clays? *Geology*, 26: 603-606.

KATZ, B., ELMORE, D.R., COGOINI, M., ENGEL, M.H. & FERRY, S., 2000. Association between burial diagenesis of smectite, chemical remagnetization, and magnetite authigenesis in the Vocontian Trough, SE France. *Journal of Geophysical Research*, 105(1): 851-868.

KLAPPER, G., FEIST, R. & HOUSE, M., 1987. Decision on the boundary stratotype for the Middle/Upper Devonian Series boundary. *Episodes*, 10/2: 97-101.

MABILLE, C. & BOULVAIN, F., 2008. Les Monts de Baileux section : detailed sedimentology and magnetic susceptibility of Hanonet, Trois Fontaines and Terres d'Haurs Formations (Eifelian / Givetian boundary and Lower Givetian, SW Belgium). *Geologica Belgica*, 11: 93-121.

MAHER, B.A., 1988. Magnetic properties of some synthetic sub-micron magnetites. *Geophysical Journal International*, 94: 83-96.

MALOOF, A.C., KOPP, R.E., GROTZINGER, J.P., FIKE, D.A., BOSAK, T., VALI, H., POUSSART, P.M., WEISS, B.P. & KIRSCHVINK, J.L., 2007. Sedimentary iron cycling and the origin and preservation of magnetization in platform muds, Andros Island, Bahamas. *Earth and Planetary Science Letters*, 259: 581-598.

PETERS, C. & DEKKERS, M.J., 2003. Selected room temperature magnetic parameters as a function of mineralogy, concentration and grain size. *Physics and Chemistry of the Earth*, 28: 659-667.

PRÉAT, A. & MAMET, B., 1989. Sédimentation de la plate-forme carbonatée givetienne franco-belge. *Bulletin des Centres de Recherche Exploration-Production Elf-Aquitaine*, 13(1) : 47-86.

PRÉAT, A., BLOCKMANS, S., CAPETTE, L., DUMOULIN, V. & MAMET, B., 2007. Microfaciès d'une lentille biohermale à la limite Eifelien/Givetien ('Fondry des Chiens', Nismes, bord sud du Synclinorium de Dinant). *Geologica Belgica*, 10: 3-25.

RIQUIER, L., AVERBUCH, O., DEVLEESCHOUWER, X. & TRIBOVILLARD, N., (2010, in press). Diagenetic versus detrital origin of the magnetic susceptibility variations in some carbonate Frasnian-Famennian boundary sections from Northern Africa and Western Europe: implications for paleoenvironmental reconstructions. *International Journal of Earth Science*.

VAN HOUTEN, F.B., 1973. Origin of red beds. A review. *Annual Review of Earth and Planetary Sciences*, 1: 39-61.

WALDEN, J., OLDFIELD, F., SMITH, J., 1999. *Environmental magnetism: a practical guide*. Technical guide n°6, Quaternary Research Association, London: 243 p.

WALLISER, O.H., BULTYNCK, P., WEDDIGE, K., BECKER, R.T. & HOUSE, M.R., 1995. Definition of the Eifelian-Givetian stage boundary. *Episodes*, 18(3): 107-115.

YAPP, C.J., 1987. Oxygen and hydrogen isotope variations among goethites (α-FeOOH) and the determination of paleotemperatures. *Geochimica et Cosmochimica Acta,* 51: 355-364.

YAPP, C.J., 1998. Paleoenvironmental interpretations of oxygen isotope ratios in oolitic ironstones. *Geochimica et Cosmochimica Acta*, 62 (14): 2409–2420.

YAPP, C.J., 2000. Climatic implications of surface domains in arrays of δD and $\delta^{18}O$ from hydroxyl minerals: Goethite as an example**.** *Geochimica et Cosmochimica Acta*, 64 (12): 2009–2025.

YAPP, C.J. & POTHS, H., 1993. The carbon isotope geochemistry of goethite (α-FeOOH) in ironstone of the Upper Ordovician Neda Formation, Wisconsin, USA: Implications for early Paleozoic continental environments. *Geochimica et Cosmochimica Acta,* 57 : 2599-2611.

ZEGERS, T.E., DEKKERS, M.J. & BAILLY, S., 2003. Late Carboniferous to Permian remagnetization of Devonian limestones in the Ardennes: role of temperature, fluids, and deformation. *Journal of Geophysical Research*, 108 (B7): 2357.

ZWING, A., MATZKA, J., BACHTADSE, V. & SOFFEL, H., 2005. Rock magnetic properties of remagnetized Palaeozoic clastic and carbonate rocks from the NE Rhenisch Massif, Germany. *Geophysical Journal International*, 160: 477-486.

Manuscript received 22.12.2009, accepted in revised form 11.05.2010, available online 15.06.2010.